.

# Intrinsic heterogeneity in liposome suspensions caused by the dynamic spontaneous formation of hydrophobic active sites in lipid membranes.

*Víctor Agmo Hernández[1]*, Göran Karlsson[1] and Katarina Edwards[1,2]*

[1]Department of Physical and Analytical Chemistry, Uppsala University, Uppsala, Sweden

[2]FRIAS, School of Soft Matter Research, University of Freiburg, Freiburg, Germany

victor.agmo@fki.uu.se

[*]V. Agmo Hernández, Department of Physical and Analytical Chemistry, Uppsala University, Husargatan 3, Box 579, 75123, Uppsala, Sweden. Phone: +46 (0) 18 471 3635. Fax: +46 (0) 18 471 3654. E-mail: victor.agmo@fki.uu.se

**Abstract**

The spontaneous, dynamic formation of hydrophobic active sites in lipid bilayer membranes is studied and characterized. It is shown that the rates of formation and consumption of these active sites control at least two important properties of liposomes: their affinity for hydrophobic surfaces and the rate by which they spontaneously release encapsulated molecules. The adhesion and spreading of liposomes onto hydrophobic polystyrene nanoparticles and the spontaneous leakage of an encapsulated fluorescent dye were monitored for different liposome compositions employing Cryo-TEM, DLS and fluorescence measurements. It was observed that an apparently homogeneous, monodisperse liposome suspension behaves as if composed by two different

populations: a fast leaking population that presents affinity for the hydrophobic substrate employed, and a slow leaking population that does not attach immediately to it. The results reported here suggest that the proportion of liposomes in each population changes over time until a dynamic equilibrium is reached. It is shown that this phenomenom can lead to irreproducibility in, e.g., spontaneous leakage experiments, as extruded liposomes leak much faster just after preparation than 24 hours afterwards. Our findings account for discrepancies in several experimental results reported in the literature. To our knowledge, this is the first systematic study addressing the issue of an existing intrinsic heterogeneity of liposome suspensions.

## 1. Introduction

Lipid vesicles, or liposomes, are self-assembled spherical lipid bilayer structures with an aqueous interior. Depending on the nature of the lipids and on the surrounding conditions, they may be anionic, cationic, zwitterionic or neutral. Liposomes are commonly used as models of biological cell membranes in studies of cell morphology, solute-membrane interaction, and other membrane-related processes (examples found in [1-4]).

Liposomes have also found important use as drug delivery vehicles, as they may contain conventional or protein/peptide drugs as well as genetic material either in their aqueous interior or embedded in the lipophilic membrane. Other applications of liposomes can be found in the cosmetic and food industries. Examples of these and other applications of liposomes have been reviewed previously [5-9].

Liposome fusion onto solid supports, pioneered by Brian and McConnell[10], can lead to the formation of supported bilayer lipid membranes (s-BLMs) which can mimic the composition of real cell membranes. These structures can be used, for example, in analyses based on several spectroscopic techniques and as biosensors based on ligand-receptor recognition at the lipid

surface[11]. On hydrophobic supports, such as mercury, the fusion of liposomes usually leads instead to the formation of adsorbed lipid monolayers[12]. These have a higher stability than s-BLMs and allow a wide range of studies on almost defect-free lipid layers.

In order to improve the potential and versatility of supported lipid mono- and bilayers, it is important to acquire a detailed understanding of the process of adhesion and spreading of liposomes on solid substrates. Several attempts have been made to explain the process in terms of the adhesion-spreading mechanism and the involved driving forces. Previous research has mainly been focused on hydrophilic solids such as silica, mica, quartz and glass (as reviewed by Richter et al[13]). A wide variety of techniques and instruments have been employed, as, for example, the quartz crystal microbalance with simultaneous frequency and dissipation measurements (QCM-D)[14-18], atomic force microscopy (AFM)[19-25], scanning force microscopy (SFM)[26], the surface force apparatus (SFA)[27], fluorescence microscopy[28,29], microcantilevers[30], surface plasmon resonance (SPR)[18,31-33] and a broad range of electrochemical methods (reviewed by Agmo Hernández and Scholz[34]). These studies have led to a good understanding of the mechanism of adhesion and spreading of liposomes on hydrophilic substrates, which consists mainly of the stages of adsorption, rupture and spreading[35,36]. On hydrophobic substrates, however, the mechanism of adhesion-spreading seems to be more complex, depending on the liposome composition and the nature of the surface and, therefore, a general consensus has not been achieved. Concerning hydrophobic metals, recent publications have proposed very convincing and widely accepted models for the mechanism leading from an adsorbed intact liposome to the formation of a supported lipid bilayer on gold[37-39] or an adsorbed lipid monolayer on mercury[40-44]. On gold, the lipid-lipid interaction is stronger than the lipid-gold interaction, and therefore a bilayer is formed. On mercury, on the other hand, the lipid-substrate interaction is the most favoured, leading to the formation of a monolayer. In spite of these differences, both models

agree that an initial rearrangement of the lipid molecules in contact with the hydrophobic surface is necessary in order for the rupture and spreading to take place. In the case of mercury, it has also been shown that not all the liposomes reaching the surface adhere to it immediately. This observation led to a recently presented model[44] that proposes that hydrophobic "active" sites must be formed on the liposome before it can adhere to the substrate. The model predicts the existence of two liposome populations near or at the surface of the substrate: an "active" population that immediately adheres and spreads on the hydrophobic surface, and an initially "inactive" population, which will sit close to the surface but will not adhere and spread. Eventually, however, these liposomes will be activated. Active liposomes are defined as those containing at least a critical amount of hydrophobic defects (active sites), and, therefore, these liposomes are referred to also as "defect liposomes". The inactive liposomes, on the other hand, do not posses a significant amount of hydrophobic defects and the entire liposome surface can in this case be considered to be hydrophilic. The model by Agmo Hernández et al.[43,44] proposes that the inactive liposomes may be reversibly activated. Due to a formal kinetic mechanism identical to that of the formation of metal nuclei on electrodes[45], this model has been called the "nucleation model"[43,44].

The way by which the activation of the liposomes takes place is not yet completely understood. It is not clear if the dynamic formation of the hydrophobic defects is an intrinsic property of the lipid membrane or if it is a consequence of its interaction with the surface. In the case of charged surfaces, it has been alleged that the electric field at the interface may trigger the formation of the hydrophobic nucleation sites, and, therefore, an induced activation has been proposed[44]. However, adhesion-spreading events have been recorded also close to the point of zero charge on a mercury electrode[46], suggesting either a spontaneous activation-deactivation process inherent to the liposomes or a different mechanism by which the surface may induce the activation.

In this report, the fusion of liposomes with similarly sized polystyrene nanoparticles in a well-mixed suspension is followed. The obtained results are conclusive concerning the nucleation model in a system controlled only by chemical kinetics and in the absence of strong electric fields. Furthermore, the role played by the predicted hydrophobic defects on other seemingly unrelated phenomena such as the rate of spontaneous leakage of the liposome contents is explored. Finally, the implications of a spontaneous inherent activation-deactivation process on the liposomes properties as a funcion of time is examined.

## 2. Materials and Methods

1-palmitoyl-2-oleoyl-*sn*-glycero-3-phosphocholine (POPC) and 1,2-dipalmitoyl-*sn*-glycero-3-phosphocholine (DPPC) were products of Avanti Polar Lipids (Alabaster, AL). NaCl, $Na_2HPO_4$, $NaH_2PO_4$ and 5(6)-carboxyfluorescein (CF) were obtained from Sigma-Aldrich (Steinheim, Germany). A sulphate stabilized aqueous suspension of polystyrene nanoparticles (PSNPs) (diameter = 115 ± 4 nm) 5% w/v was obtained from microParticles Gmbh (Berlin, Germany). All reagents were used as received. Aqueous solutions were prepared using deionized water (18.4 MΩ cm) obtained from a Milli-Q system (Millipore, Bedford, USA).

*Liposome preparation*

The desired lipid was dissolved in $CHCl_3$ and the solvent was removed under a gentle nitrogen stream. The remaining $CHCl_3$ was removed in vacuum. The resulting lipid films were then hydrated either with a phosphate buffer saline (PBS, 10 mM phosphate, 150 mM NaCl, pH=7.4) for the cryotransmission electron microscopy (cryo-TEM), dynamic light scattering (DLS) and turbidity measurements; or with a 100 mM CF solution in 10 mM phosphate (pH = 7.4 and isoosmolar with the PBS) for the leakage measurements. The films were suspended by vortexing and subjected to five freeze-thaw cycles. The suspension was then extruded 31 times through a

polycarbonate filter of pore size 100 nm using a Lipo-Fast extruder (Avestin, Ottawa, Canada), keeping the temperature above the main phase transition temperature of the lipid used. The time at which the extrusion was completed was recorded for all prepared suspensions. The liposomes thus obtained were characterized by DLS and cryo-TEM, confirming that the resulting suspensions were composed mainly on unilamellar vesicles with an average diameter of 100 nm.

*Leakage experiments*

The measurements were performed under constant stirring at 25 ºC with a SPEX fluorolog 1650 0.22-m double spectrometer (SPEX industries, Edison, NJ). The excitation and emission wavelengths were set to 495 and 520 nm respectively. The fluorescence intensity was recorded every 5 seconds unless stated otherwise.

The liposome suspensions prepared in CF buffer were gel filtrated over a PD-10 desalting column from Amershan Biosciences (Uppsala, Sweden) in order to separate the untrapped CF buffer from the liposomes, replacing it with PBS. The time elapsed between the extrusion and the end of the separation was recorded, as well as the time elapsed from the separation until the start of the leakage measurements. When curve fitting on spontanous leakage curves was performed, the fitting parameters were extrapolated to account for this latter time. The suspension was diluted to a final concentration of 12 μM lipid, in order to keep the concentration dependent fluorescence signal from the released CF within the linear range. In order to normalize the obtained data with respect to the total amount of trapped CF, a volume of 50 μL of a 100 mM Triton X-100 solution was added to the samples after each experiment and the fluorescence intensity at complete leakage was recorded. The degree of leakage was calculated over time according to:

$$x_{\mathrm{CF_{Released}}}(t) = \left(I(t) - I_0\right) \Big/ \left(I_{total} - I_0\right) \qquad (1)$$

where $I(t)$ is the time dependent recorded intensity, $I_0$ is the intensity at the beginning of the experiment and $I_{total}$ is the intensity measured after adding Triton X-100 to the suspension. The signal was recorded for at least 5 and up to 24 hours.

Both the spontaneous CF leakage and the CF release upon liposome adhesion and rupture on PSNPs were followed. For the latter experiments, a large excess of PSNPs (final particle surface area/lipid surface area ratio between 5 and 15) was added to the liposome suspension a short time (60-100 s) after the measurement had started. A sudden increase in the fluorescence intensity was observed upon addition of the particles, caused by the large amount of light scattered by the PSNPs. The magnitude of this increase was determined by adding different volumes of the original PSNPs suspension to a CF solution and recording the observed intensity jumps. The fluorescence signal after additon of the particles to the liposome suspension was corrected according to these results in order to substract the scattering contribution from the overall signal. Furthermore, the first 100 s after addition of the particles were not considered in the subsequent analysis, in order to ensure complete mixing and a stable fluorescence signal.

*Effect of the "maturing time" on the rate of spontaneous leakage of liposomes*.

The spontaneous leakage of CF entrapped in the liposomes was followed as described above. For a single batch of liposomes, several aliquotes (at least four) were taken and each was separated from the untrapped CF at different times after extrusion. The time between separation and the beginning of the measurement was kept constant for each batch (between 30 and 45 min). The purpose was to monitor the effect of liposome age ("maturing time") on the spontaneous leakage rate.

*Cryo-TEM studies*

Cryo-TEM studies were performed with a Zeiss EM 902A transmission electron microscope (Carl Zeiss, Oberkochen, Germany) operating at 80 kV and in zero-loss bright-field mode. Digital images were recorded under low-dose conditions with a BioVision Pro-SM Slow Scan CCD camera (Proscan, Scheuring, Germany). The method for sample preparation has been described in detail by Almgren et al.[47]. The lipid concentrations used were between 0.5 and 1.5 mM.

*Light scattering measurements*

The size distribution of the liposome suspensions was monitored by means of dynamic light scattering. The light source used was a Uniphase He-Ne laser emitting vertically polarised light at a wavelength of 638.2 nm and operating at 25 mW. Data were collected at 25 ºC and scattering angle 90º using a PerkinElmer (Quebec, Canada) diode detector connected to an ALV-5000 multiple digital autocorrelator (ALV-laser Vertriebsgesellschaft mbH, Germany). The lipid concentration in the samples was between 0.5 and 1 mM.

For the PSNPs-liposome mixtures, the changes in size distribution over time were followed both by using the set up described above and by employing a Nicomp 380 (Particle Sizing Systems, USA) at 23 ºC using disposable plastic cuvettes. The lipid concentration used was 12 μM.

*Turbidity measurements*

Optical density measurements were performed with liposome-PSNPs mixtures, lipid concentration 12 μM, at 23 ºC using an HP 8453 absorbance spectrophotometer (Hewlett Packard, Böblingen, Germany) at a wavelength of 600 nm.

## 3. Results and discussion

### *3.1 Adhesion and spreading of DPPC liposomes on PSNPs*

Figure 1 shows the CF leakage curve obtained when a 12 μM DPPC liposome suspension is mixed with 5 times area excess of PSNPs. Based on previous reports[40-42,44], it is assumed that all processes involved in the adhesion-spreading process follow first or pseudofirst order kinetics. One should then be able to fit the experimental curve to a sum of exponential terms. To determine the optimal number of terms describing the experimental curve without overparameterizing, a series of fits were performed, starting from a single exponential term and adding extra terms one at a time while performing significance t-tests for each new term. The best fitting was obtained with three exponential terms:

$$x_{\mathrm{CF_{Released}}}(t) = 1 + C_1 e^{-t/\tau_1} + C_2 e^{-t/\tau_2} + C_3 e^{-t/\tau_3} \qquad (2)$$

with all six fitting parameters being significant according to the t-test ($p < 0.001$).

Figure 1 shows the good agreement between the experimental and the fitted curves. The three terms exponential curve agrees well with the nucleation model, which proposes the following mechanism of activation-adhesion-spreading:

$$\mathrm{L_i} \underset{k_b}{\overset{k_a}{\rightleftarrows}} \mathrm{L_a} \xrightarrow{k_1*[\mathrm{PS}]} \mathrm{N} \xrightarrow{k_2} \mathrm{L_f} \qquad (\mathrm{I})$$

where a large excess concentration of PSNPs ([PS]) is assumed, N represents the species formed by an intact liposome attached to a particle (a nucleus), $L_f$ represents the fused liposome, $L_i$ and $L_a$ are the inactive and active liposomes respectively, $k_a$ and $k_b$ are the activation and deactivation rate constants, respectively, $k_1*[\mathrm{PS}]$ is the actual "nucleation" pseudofirst order rate constant and $k_2$ is the rate constant comprising the steps leading from an adhered liposome to an spread adsorbed lipid monolayer (which cannot be resolved by the experiment described here). In terms of the path followed by the entrapped CF, mechanism (I) can be rewritten as:

$$\begin{array}{l} \mathrm{CF(L_i)} \underset{k_b}{\overset{k_a}{\rightleftarrows}} \mathrm{CF(L_a)} \xrightarrow{k_1^*[\mathrm{PS}]} \mathrm{CF(N)} \xrightarrow{k_2'} \mathrm{CF_{Response}} \\ \downarrow k_{L1} \qquad\qquad \downarrow k_{L2} \\ \mathrm{CF_{Response}} \qquad \mathrm{CF_{Response}} \end{array} \qquad \text{(II)}$$

where CF($i$) represents the amount of CF trapped in each of the species, and $\mathrm{CF_{response}}$ represents the leaked or released fluorophore producing a fluorescence response. The fluorescence signal would then arise due to four contributions: the spontaneous leakage of the inactive and the active liposomes, given respectively by $k_{L1}$ and $k_{L2}$ (which may have different values), the spontaneous leakage of the intermediate N, and the leakage caused by the rupture of the liposomes in order to spread. These last two processes cannot be analytically separated from one another and are therefore represented together with a rate constant $k_2'$. Solving the kinetic equations involved in mechanism II, the response will be given by:

$$x_{\mathrm{CF_{Released}}}(t) = \left( \begin{array}{l} 1 + \left( \dfrac{A-\lambda-P}{2\lambda} + \dfrac{X}{(A+\lambda-2B)\lambda} \right) e^{-\frac{A+\lambda}{2}t} \\ -\left( \dfrac{A+\lambda-P}{2\lambda} + \dfrac{X}{(A-\lambda-2B)\lambda} \right) e^{-\frac{A-\lambda}{2}t} \\ + \dfrac{2X}{(A-\lambda-2B)(A+\lambda-2B)} e^{-Bt} \end{array} \right) \qquad (3)$$

where $A = k_a + k_b + k_1^*[\mathrm{PS}] + k_{L1} + k_{L2}$, $P = 2\left(k_{L1}x^0_{\mathrm{CF_{L_i}}} + k_{L2}x^0_{\mathrm{CF_{L_a}}}\right)$, $B = k_2'$,

$\lambda^2 = \left(k_a - k_b - k_1^*[\mathrm{PS}] + k_{L1} - k_{L2}\right)^2 + 4k_a k_b$, $X = 2k_1^*[\mathrm{PS}]\left(k_2' x^0_{\mathrm{CF_{L_a}}} + k_{L1}x^0_{\mathrm{CF_{L_i}}} - k_a - k_{L1}\right)$ and $x^0_{\mathrm{CF_{L_a}}}$ and $x^0_{\mathrm{CF_{L_i}}}$ are the initial fractions of total CF inside the active and the inactive liposomes respectively. These initial conditions are unique for each experiment, as they depend on the time elapsed since the extrusion, the interval since the separation, as well as on the initial fraction of

active liposomes, which cannot be guaranteed to be the same for all liposome preparations. Equation 3 corresponds well with the experiment, and the values of $A$, $B$, $X$, $P$ and $\lambda$ can be estimated from the fitting parameters in equation 2 given the relationships: $A = \tau_1^{-1} + \tau_3^{-1}$, $\lambda = \tau_1^{-1} - \tau_3^{-1}$, $B = \tau_2^{-1}$ and the preexponential factors in equation 2 being equivalent to those in equation 3. Notice that the corresponding values of $\tau_1$, $\tau_2$ and $\tau_3$ can be arbitrarily assigned to any of the time constants obtained from the curve fitting. An immediate objective determination of the desired parameters is therefore not possible under these circumstances. This problem will be addressed in section 3.2. Furthermore, although the model described by equation 3 fits very well to the experimental data, there is an unlimited number of mechanisms that would give rise to a three term exponential equation and would therefore fit just as well. Besides this, in the terms it is written, the mechanism assumes that the activation-deactivation equilibrium is independent of the presence and concentration of PSNPs. If that is the case, evidence for such equilibrium should be found in an undisturbed liposome suspension.

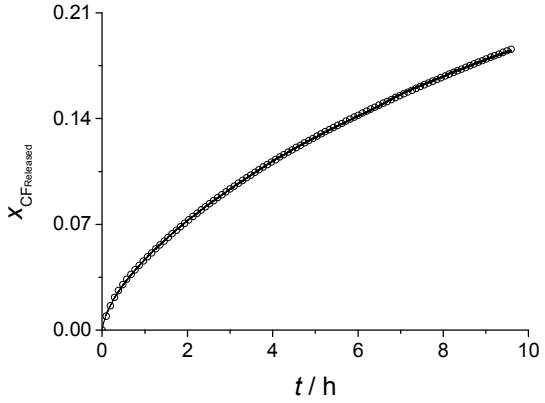


**Figure 1.** Leakage curve obtained from a mixture of CF loaded DPPC liposomes (100 nm, 12 μM lipid) and PSNPs 115 nm (5 times area excess) at 25 ºC. Solid line: experimental data. Empty circles: Three-term exponential fitting curve (Adjusted $R^2$ = 0.99993, $p < 0.001$ for all fitting parameters).

*3.2.Spontaneous leakage of CF from DPPC liposomes*

By measuring the spontaneous leakage of CF from the liposomes, it was observed that the experimental curve after long (several hours) measurement times is best described by two exponential terms ( $x_{\mathrm{CF_{Released}}}(t) = 1 + C_1' e^{-t/\tau_1'} + C_2' e^{-t/\tau_2'}$ ) (Adjusted $R^2$ = 0.99873, $p < 0.001$ for all fitting parameters), which would agree with the mechanism:

$$\mathrm{CF_{response}} \xleftarrow{k_{L1}} \mathrm{CF(L_i)} \underset{k_b}{\overset{k_a}{\rightleftharpoons}} \mathrm{CF(L_a)} \xrightarrow{k_{L2}} \mathrm{CF_{response}} \qquad \text{(III)}$$

which is the starting assumption of the nucleation model. The experimental curve would then be described by the equation:

$$x_{\mathrm{CF_{Released}}}(t) = 1 + \left(\frac{A' - \lambda' - P}{2\lambda'}\right) e^{-\frac{A'+\lambda'}{2}t} - \left(\frac{A' + \lambda' - P}{2\lambda'}\right) e^{-\frac{A'-\lambda'}{2}t} \qquad (4)$$

where $A' = k_a + k_b + k_{L1} + k_{L2}$, $\lambda'^2 = \left(k_a - k_b + k_{L1} - k_{L2}\right)^2 + 4k_a k_b$ and $P$ has the same values as in equation 3. The values of $A'$ and $\lambda'$ can be estimated from the fitting parameters according to the relationships: $A' = \tau_1'^{-1} + \tau_2'^{-1}$ and $\lambda' = \tau_1'^{-1} - \tau_2'^{-1}$. In this case, the values of the obtained fitting parameters can be assigned unequivocally to $\tau_1'$ and $\tau_2'$, as it is clear that, in order to keep $\lambda'$ positive, $\tau_1' < \tau_2'$ should hold. Averaged from 25 measurements, the obtained values are $A' = 2.07 \times 10^{-4} \pm 4.5 \times 10^{-5}\ \mathrm{s}^{-1}$ and $\lambda' = 2 \times 10^{-4} \pm 4.46 \times 10^{-5}\ \mathrm{s}^{-1}$ (error margins given in terms of the standard error).

From the data obtained, it is also possible to assign the corresponding fitting values to $\tau_1$, $\tau_2$ and $\tau_3$ in equation 2. It is clear that $A > A'$, and, as the values of the three time constants obtained from the fitting differ several orders of magnitude (from $10^5$ to $10^2$ s), this is only possible if $\tau_1 < \tau_1'$. This allows assigning unequivocally the smallest time constant obtained from the fitting as the value of $\tau_1$. Two time constants are left, one being in the order of $10^5$ s. Based on previous studies of liposome adhesion-spreading, it is unlikely that the leakage and consumption of the nuclei N is so slow as to correspond to that large time constant. Therefore, it is assumed that this value corresponds to $\tau_3 = 2\left(A - \lambda\right)^{-1}$. The remaining time constant is then assigned to $\tau_2 = B^{-1}$.

*3.3.Effect of liposome age on the spontaneous leakage rate.*

By measuring the spontaneous leakage of a batch of DPPC liposomes at different times after extrusion, but at a constant time after separation from the untrapped CF, it is possible to show that the liposome suspension is changing over time ("maturing"). Figure 2 shows that freshly prepared liposomes leak more of their contents than older ones in the same period of time. When

fitting the curves to a two exponential equation, it is revealed that this trend is reflected mainly in the pre-exponential factors $C_1'$ and $C_2'$, while the time constants $\tau_1'$ and $\tau_2'$ are distributed randomly around an average value, as can be seen in Table 1. The pre-exponential factors are related to the initial conditions of the experiment and thus the experiment shows that those conditions change over time. The size distribution of the liposome suspension as determined by DLS follows a lognormal distribution and the mean radius remains constant and independent of the elapsed maturing time, as shown in Table 2, discarding the posibility that the observed changes arise from liposome-liposome fusion. According to the nucleation model, the observed changes may arise due to the fact that the preparation initially contains a higher than equilibrium proportion of active liposomes. This proportion decays over time until the equilibrium is reached. By definition, the active liposomes present a high concentration of hydrophobic defects. According to the data presented here, these defects would not only increase the affinity of the liposomes for hydrophobic substrates, but would also cause a faster leakage of the liposome contents. Interestingly, the data suggests that the process of formation and consumption of such defects occurs dynamically in a liposome suspension, giving rise to a certain and unavoidable degree of heterogeneity in an otherwise homogeneous suspension.

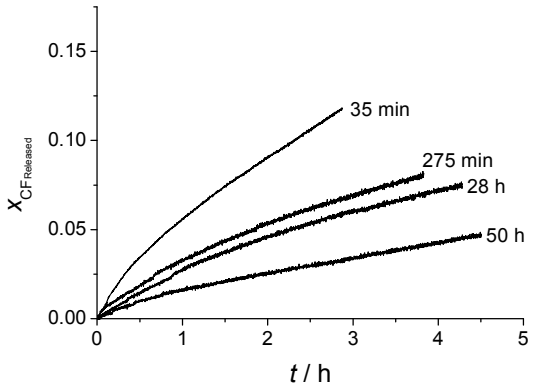


**Figure 2.** Effect of the liposome maturing time on the spontaneous leakage of CF from DPPC liposomes at 25 ºC.

**Table 1.** Fitting parameters for the experimental curves displayed in Figure 2 showing the effect of the maturing time on the spontaneous leakage behaviour. Error values are the standard errors determined from the fitting procedure.

| Maturing time | $C_1'$ | $C_2'$ | $\tau_1'$ / s | $\tau_2'$ / s |
|---|---|---|---|---|
| 35 min | $-0.0792 \pm 6.99 \times 10^{-4}$ | $-0.9208 \pm 6.91 \times 10^{-5}$ | $1427.4 \pm 9.4$ | $1.02 \times 10^5 \pm 85$ |
| 5 h | $-0.0443 \pm 4.05 \times 10^{-4}$ | $-0.9557 \pm 4.44 \times 10^{-4}$ | $2902 \pm 65.4$ | $2.26 \times 10^5 \pm 2012$ |
| 28 h | $-0.0450 \pm 9.79 \times 10^{-4}$ | $-0.9550 \pm 1.02 \times 10^{-3}$ | $4550 \pm 138.4$ | $3.01 \times 10^5 \pm 6301$ |
| 50 h | $-0.0226 \pm 1.09 \times 10^{-4}$ | $-0.9774 \pm 1.22 \times 10^{-4}$ | $1925.4 \pm 48$ | $4.24 \times 10^5 \pm 2268$ |

**Table 2.** Mean liposome radius ( $\overline{R}$ ) and standard deviations (*s*) as a function of the maturing time as determined by DLS for 0.5 mM DPPC liposome suspensions.

| Maturing time | $\overline{R}$ / nm | *s*/ nm |
|---|---|---|
| 35 min | 49.3 | 0.19 |
| 5 h | 51.7 | 0.25 |
| 28 h | 47.4 | 0.23 |
| 50 h | 47 | 0.26 |

A plot of the preexponential factors $C_1^{'}$ and $C_2^{'}$ obtained from the fitting of the experimental data against the maturing time provides with information concerning the activation-deactivation process. If mechanism III is true, it can be shown that the parameter $C_1^{'}$ as a function of the maturing time is given by:

$$C_1^{'}\left(t_{\mathrm{m}}\right) = Z - Ye^{-\left(k_{\mathrm{a}}+k_{\mathrm{b}}\right)*t_{\mathrm{m}}} \qquad (5)$$

where $t_{\mathrm{m}}$ is the maturing time, $Z = \left(A^{'} - \lambda^{'}\right)\Big/\left(2\lambda^{'}\right) - \left(k_{\mathrm{L1}}k_{\mathrm{b}} + k_{\mathrm{L2}}k_{\mathrm{a}}\right)\Big/\left(\left(k_{\mathrm{a}} + k_{\mathrm{b}}\right)\lambda^{'}\right)$, $Y = k_{\mathrm{L1}}k_{\mathrm{L2}}\left(k_{\mathrm{a}}x_{\mathrm{L_i}}^{0} - k_{\mathrm{b}}x_{\mathrm{L_a}}^{0}\right)\Big/\left(\left(k_{\mathrm{a}} + k_{\mathrm{b}}\right)\lambda^{'}\right)$ and $x_{\mathrm{L_a}}^{0}$ and $x_{\mathrm{L_i}}^{0}$ are the proportions of active and inactive liposomes just after extrusion, respectively.

Figure 3 shows the evolution of $C_1^{'}$ over maturing time for two different liposome batches of the same composition (pure DPPC) and at the same temperature. It can be seen that the initial conditions differ greatly between batches, even though the preparation procedure is the same. This difference in composition may arise from small, overlooked differences in the preparation procedure, such as the extrusion pressure (which, in the method employed here, cannot be guaranteed to be the same for all liposome batches). However, both sets of data can be fitted to

equation 5, sharing a single value for the relaxation constant ($k_a + k_b = 6.718 \times 10^{-5} \pm 3.29 \times 10^{-5}$ $s^{-1}$) and for the limiting conditions (given by $Z = 0.02318 \pm 0.0032$).

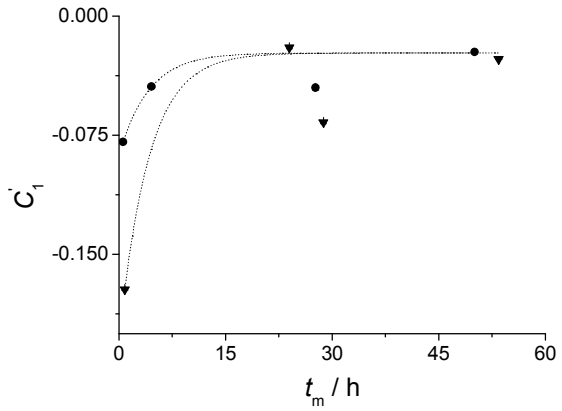


**Figure 3.** Pre-exponential factor $C_1'$ as a function of the maturing time for two different DPPC liposome batches kept at 25 ºC. The values represented by circles correspond to the same batch as Figure 2. The dotted lines represent the curve fittings according to equation 5 (global fit, instrumental weighting).

*3.4.Tuning of the pseudo first order nucleation rate constant*

In order to show the connection between, on the one hand, the fast leaking and slow leaking liposomes and, on the other hand, the active-inactive liposome exchange controlling the affinity for hydrophobic surfaces we need to go back to equation 3. The pseudo first order rate constant $k_1 * [\mathrm{PS}]$ can be tuned by changing the concentration of added PSNPs, and the changes should be reflected in the curve fitting parameters. A plot of the parameter $A$ vs. [PS] should fit to a line with a slope equal to the second order rate constant $k_1$ and, if the exchange between fast leaking and slow leaking liposomes is equivalent to the exchange between active and inactive liposomes, the intercept on the $A$ axis should be equal to $A'$ in equation 4. In fact, as shown in Figure 4, a

good linear correlation is obtained upon plotting the value of $A'$ and the values of $A$ obtained at different [PS]. The determined slope is $k_1 = 4.32 \times 10^{-15}$ mL*particles$^{-1}$*s$^{-1}$, and the y-intercept is $2.7944 \times 10^{-4}$ s$^{-1}$ $\approx A'$. It can be seen that at large values of [PS] ($S_{PSNP}/S_{DPPC}$ = 15, where $S$ is the surface area of the species) the obtained values of $A$ present a very large variance. At such high nanoparticle concentration it is likely that the adhesion reaction is not confined to the one liposome-one particle process assumed by equation 3. Several particles may attach to the liposome at the same time, and particle-particle interactions may take place in a way not always reproducible, leading to the large observed variation. As will be shown in sections 3.6 and 3.8 this behaviour is always observed when POPC liposomes are employed. As an instrumental weighting is employed for the linear fitting, this point barely contributes to the final result.

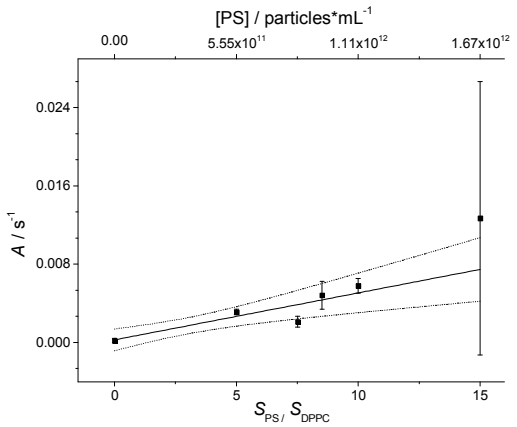


**Figure 4.** Plot of $A$ vs. the added concentration of PSNPs ([PS]). The pointed lines delimit the 95% confidence area for a linear fitting. Error bars are given by the standard deviation calculated from at least two repetitions of the measurements. Each point in the plot has a specific weight equal to the reciprocal of its variance (instrumental weight).

From the values of $A'$, $\lambda'$, $B$, $Z$, the relaxation constant $k_a + k_b$, and from the plot shown in Figure 4, it is possible to estimate the rate constants involved in the nucleation process. The

activation-deactivation rates and the rate of formation of the nucleus, as well as the rates of spontaneous leakage for active and inactive liposomes can be determined. A summary of the results is shown in Table 3, including the calculated value of the activation-deactivation equilibrium constant $K = k_a/k_b$ and the expected proportion of inactive liposomes at equilibrium $x_L^{eq}$.

**Table 3.** Rate constants describing the activation-deactivation, CF spontaneous leakage and adhesion-spreading of DPPC liposomes on PSNPs at 25 ºC according to the nucleation model.

| $k_a$ / $10^{-5}$ $s^{-1}$ | $k_b$ / $10^{-5}$ $s^{-1}$ | $k_{L1}$ / $10^{-5}$ $s^{-1}$ | $k_{L2}$ / $10^{-5}$ $s^{-1}$ | $k_1$ [a] / $10^{-15}$* [PS]$^{-1}$ $s^{-1}$ | $k_2'$ /$10^{-5}$ $s^{-1}$ | $K$ | $x_L^{eq}$ |
|---|---|---|---|---|---|---|---|
| .338 ± .325 | 6.38± 2.93 | .069 ± 3.16 | 13.9 ± 4.41 | 4.32 ± .647 | 13.8 ± 6.11 | 0.053 | 0.95 |

[a][PS] given in particles*$mL^{-1}$

The accuracy of the nucleation model and of the kinetic parameters presented in Table 3 is further proved by the results from DLS and Cryo-TEM investigations. Given the low value of $k_2'$, it is expected that the intermediate (the nucleus "N") will remain relatively stable before the lipid bilayer eventually ruptures and spreads. In order to detect this intermediate N, a mixture 1:1 (particle count) of DPPC liposomes and PSNPs was observed at different reaction times using cryo-TEM and DLS. To ensure that the active-inactive populations have reached equilibrium, the liposomes were left to mature for 48 hours before mixing with the nanoparticles. At a concentration of 1 mM DPPC and under the prevalent conditions, it is expected that the concentration of N will reach a maximum 4 minutes after mixing (as estimated from chemical kinetics simulations). Figure 5a shows that, at that time, intact liposomes attached to particles are observed in the cryo-TEM pictures and their presence is confirmed by an increase in the particle

radius as determined by DLS. After longer times, the population of the intermediate decreases until it cannot be detected by the methods employed. Figure 5b shows also some liposome-particle complexes in the process of spreading. As the total lipid area per liposome is larger than the area of a PSNP, a certain amount of excess lipid remains unspread. Observing the mixture at longer times, it is observed that this lipid excess is dettached as small liposomes (Figure 5c). No significant changes in the turbidity of the suspension are observed over time (data not shown). As turbidity arises mainly from PSNPs, this result suggests that no aggregation of particles occurs, consistent with the DLS measurements and suggesting that the liposome-particle adhesion-spreading process follows a one liposome-one particle mechanism, as assumed in mechanism II.

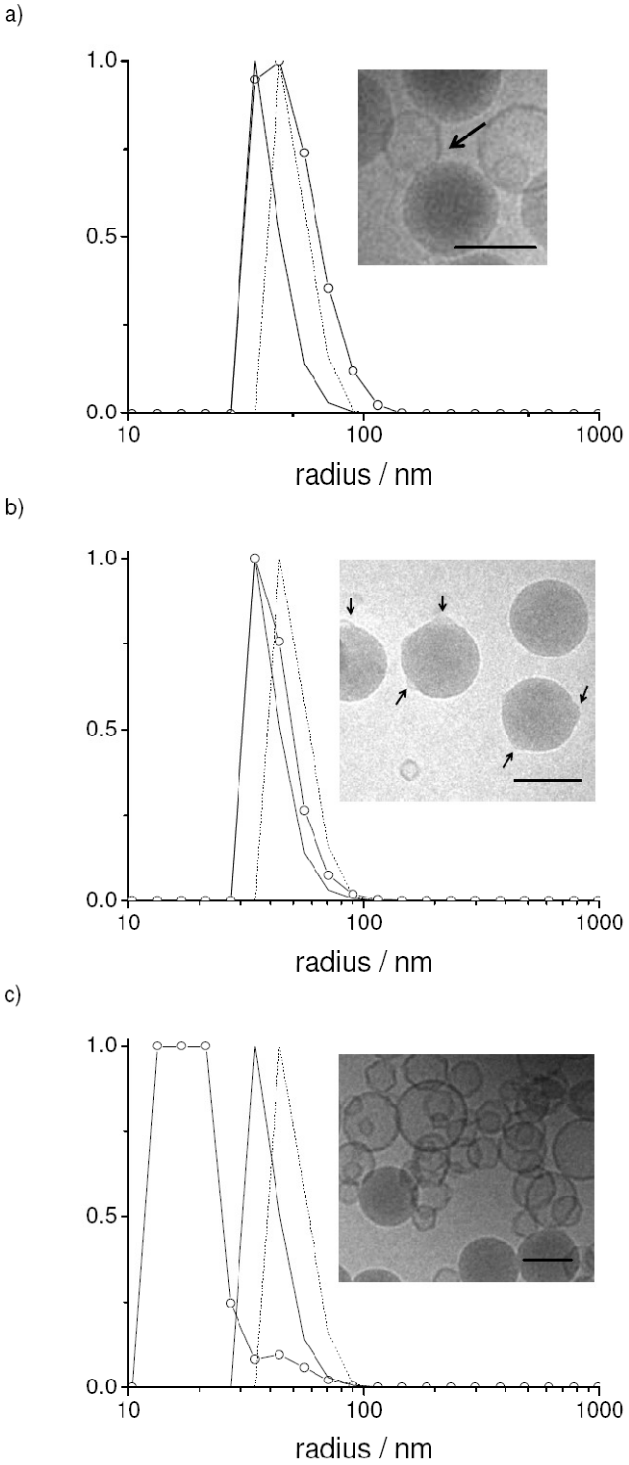


**Figure 5.** Particle size distributions (number weighted) obtained by DLS and cryo-TEM pictures (bar = 100 nm) of different stages of the DPPC liposome adhesion-spreading on PSNPs (1 mM DPPC 1:1 liposome-particle mixture). Solid lines: pure DPPC liposomes. Dotted lines: pure

PSNPs. Connected open circles: Mixture shown in the picture: a) 4 minutes after mixing, the arrow points an intermediate (nucleus, a liposome attached to a particle), b) 24 hours after mixing. Lipid bilayer bumps are observed on the surface of the particles, c) 48 h after mixing. Small unilamellar vesicles appear, presumably from the excess lipid dettaching from the particles.

### *3.5.Sequential PSNP and liposome additions*

The results and analysis on CF leakage presented above rely heavily on the non-linear fitting of the experimental curves and on the proposed interpretation of the fitting parameters. This leaves open the discussion about the validity of the assumptions employed to develop the fitting model. Further experiments were designed to show, without the need of referring to the mathematical model, that only a fraction of matured DPPC liposomes in a suspension present affinity for the PSNPs. First, the CF release from a 6-1 PSNPs-DPPC surface area mixture was monitored until the rate of release remained constant in the employed time-scale (approximately two hours). Secondly, the required volume of a concentrated PSNPs suspension was added to the mixture in order to double the concentration of PSNPs, and the CF release was followed for another 20 minutes. Afterwards, liposomes from a more concentrated suspension were added in order to double the liposome concentration on the sample and the CF release was again monitored for 30 minutes.

Figure 6 shows the CF release profile of the mixture and how it changes when the additions are made. After 2.5 h, the 6-1 mixture CF release rate is constant and only approximately 1 % of the total CF has been released. This clearly indicates that most liposomes are intact and have not yet fused with the polymer nanoparticles. In spite of the large amount of non-reacted liposomes still present in the suspension, the addition of an extra amount of PSNPs does not have any

measurable effect on the release rate. On the other hand, when adding an extra amount of liposomes, the release profile resembles the fast leakage observed during the first minutes of the experiment. This can be clearly observed in the inset on Figure 6, where the three sections of the experiment are compared in the same time scale. Addition of extra liposomes "resets" the experiment, i.e., the response is the same as when the experiment was started.

These observations show that the limiting step in the adhesion reaction of liposomes on PSNPs does not involve the latter. Furthermore, they show that a fraction of the CF is released promptly from DPPC liposomes both in a fresh mixture and upon addition of more liposomes to an already existent mixture. The interpretation of these results is that a small fraction of the liposomes react readily with the PSNPs while the rest of them remain intact in suspension. This assumption agrees completely with the release profile shown in Figure 6. The fact that the released CF signal continues to increase at longer times (although at a slower rate and with kinetics different than for spontaneous leakage), implies that the intact liposomes eventually adhere and spread on the particles. All these observations provide further, purely experimental evidence supporting the nucleation model of DPPC liposomes on PSNPs.

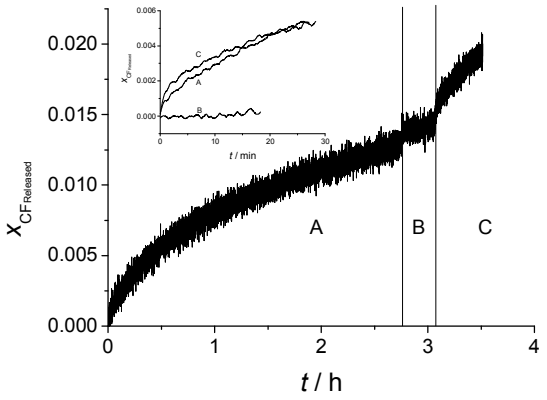


**Figure 6.** CF release profile (sampling each second) of A) a 6-1 PSNPs – DPPC liposomes surface area mixture at 25 ºC, B) after doubling the PSNPs concentration and C) after doubling

the liposome concentration. The inset shows a comparison of the smoothed curves for the three sections plotted on their own time and CF release scales.

### *3.6. Adhesion-spreading of POPC liposomes in the liquid-crystalline phase state onto PSNPs*

Figure 7 shows a comparison between the spontanous leakage of CF from matured (30 hours) POPC liposomes and the leakage observed in a mixture of POPC liposomes (same maturing time) and PSNPs using 5 and 8.5 times PSNPs excess area. Surprisingly, it is observed that the addition of PSNPs prevents the leakage of CF instead of increasing it by means of the adhesion-spreading process. The fitting curves show that the spontaneous leakage can be modelled in the same way as for DPPC. The leakage upon addition of PSNPs, however, presents a small but significant difference when compared to the case of DPPC liposomes: even though the experimental curve is also fitted to a three-term exponential equation, the limiting value (i.e. the estimated proportion of CF released after an infinite time) does not reach unity. In other words, a certain amount of the CF remains trapped inside the liposomes, with no mechanism by which it can leak. As no liposome is capable of 100% retention over long periods, it is necessary to assume that a new kind of entity is formed that encapsulates intact liposomes and inhibits the leakage of CF. These proposed entities, however, do not resist the attack of Triton X-100 as, after addition of the detergent, the fluorescence signal reaches the expected value for complete leakage. As Figure 7 shows, at increasing concentrations of PSNPs, the limiting value of the fluorescence signal is diminished, suggesting that the leakage inhibiting entity is formed, at least partially, by the polymer particles.

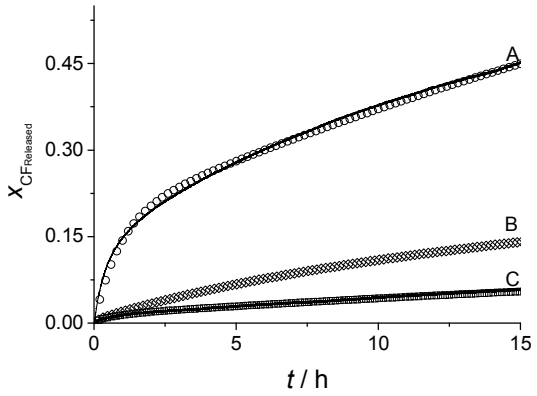


**Figure 7.** (A) CF spontaneous leakage from mature (30 h) POPC liposomes and leakage upon mixture with 5 (B) and 8.5 (C) times excess PSNPs surface area. Solid lines: experimental data. Open symbols: fitted curves A) two-terms exponential equation and B-C) three-terms exponential equation.

It is therefore plausible to assume that the inhibitor is formed by a liposome surrounded by a cluster of PSNPs (data supporting this hypothesis is presented in section 3.8 below). The CF contained in the liposome would be released to the bulk solution at a very slow rate, not measurable at the time scale of the experiment. For practical purposes, this leakage can be considered to be non-existent. An accurate adhesion-spreading mechanism of POPC on PSNPs should in this case include the formation of the inhibitor, as follows:

$$\begin{array}{l} L_i \underset{k_b}{\overset{k_a}{\rightleftharpoons}} L_a \xrightarrow{k_1*[PS]} N \xrightarrow{k_2'} L_f \\ \qquad\quad \downarrow\ k_I*[PS]^n \\ \qquad\quad I \end{array} \qquad \text{(IV)}$$

where I represents the inhibitor, $k_I$ the rate constant of its formation and $n$ an unknown order parameter, with all other symbols having the same meaning as described above. This model is coined the nucleation-inhibition mechanism.

In terms of the trapped CF, mechanism IV becomes:

$$\begin{array}{ccccccc} \mathrm{CF_{Response}} & & \mathrm{CF_{Response}} & & & & \\ \uparrow k_{L1} & & \uparrow k_{L2} & & & & \\ \mathrm{CF(L_i)} & \underset{k_b}{\overset{k_a}{\rightleftarrows}} & \mathrm{CF(L_a)} & \xrightarrow{k_1*[\mathrm{PS}]} & \mathrm{CF(N)} & \xrightarrow{k_2'} & \mathrm{CF_{Response}} \\ & & \downarrow k_1*[\mathrm{PS}]^n & & & & \\ & & \mathrm{CF(I)} & & & & \end{array} \qquad \text{(V)}$$

which results in a response profile given by:

$$x_{\mathrm{CF_{Released}}}(t) = \left( \begin{array}{l} 1 + \dfrac{2W}{\left(A'' + \lambda''\right)\left(A'' - \lambda''\right)} + \left( \dfrac{A'' - \lambda'' - P}{2\lambda''} + \dfrac{X}{\left(A'' + \lambda'' - 2B\right)\lambda''} + \dfrac{W}{\left(A'' + \lambda''\right)\lambda''} \right) e^{-\frac{A'' + \lambda''}{2}t} \\ -\left( \dfrac{A'' + \lambda'' - P}{2\lambda''} + \dfrac{X}{\left(A'' - \lambda'' - 2B\right)\lambda''} + \dfrac{W}{\left(A - \lambda''\right)\lambda''} \right) e^{-\frac{A'' - \lambda''}{2}t} \\ + \dfrac{2X}{\left(A'' - \lambda'' - 2B\right)\left(A'' + \lambda'' - 2B\right)} e^{-Bt} \end{array} \right)$$

(6)

where $W = 2k_1 * [\mathrm{PS}]^n \left(k_{L1} x^0_{\mathrm{CF_{L_i}}} - k_a - k_{L1}\right)$, $A'' = k_a + k_b + k_1 * [\mathrm{PS}] + k_{L1} + k_{L2} + k_I * [\mathrm{PS}]^n$,

$\left(\lambda''\right)^2 = \left(k_a - k_b - k_1 * [\mathrm{PS}] + k_{L1} - k_{L2} - k_I * [\mathrm{PS}]^n\right)^2 + 4k_a k_b$, and $X$, $P$ and $B$ have the same values as for equation 3. Equation 6 corresponds well with the observed experimental curves, and accounts for the lower leakage of the liposomes when mixed with PSNPs.

*3.7. Maturing of POPC liposomes*

As in the case of DPPC, the discussion above assumes a spontaneous process of activation-deactivation and a relationship between fast leaking liposomes and liposomes with affinity for hydrophobic surfaces. If this is true, POPC liposomes should also "mature" over time. At first sight, however, there is no apparent trend observed in the spontaneous leakage of CF for a batch

of POPC liposomes measured at different maturing times, as shown in Figure 8. At the same time, the experiment is not reproducible, with significant, apparently aleatory, changes occurring over time. By fitting the experimental curves according to equation 2 it is obvious, however, that the pre-exponential factors do follow a clear trend, as shown in Table 4. The observed behavior of the preexponential factors is expected from an activation-deactivation process, and can be described as a function of the time elapsed since extrusion according to equation 5, as shown in Figure 9. As POPC liposomes leak faster than DPPC liposomes, the time elapsed between the separation of the liposomes from the untrapped CF and the start of the measurements has a more pronounced impact on the experimental curve, leading to the apparent random trend observed in Figure 8. However, as Table 4 shows, once the data is extrapolated to consider the time between the separation and the experiment, the expected exponential changes in the preexponential factor are observed. The relaxation constant thus calculated is equal to $k_a + k_b = 3.41 \times 10^{-5} \pm 1.12 \times 10^{-5}$ $s^{-1}$, while the estimated limiting conditions are given by $Z = 0.27868 \pm 0.00337$.

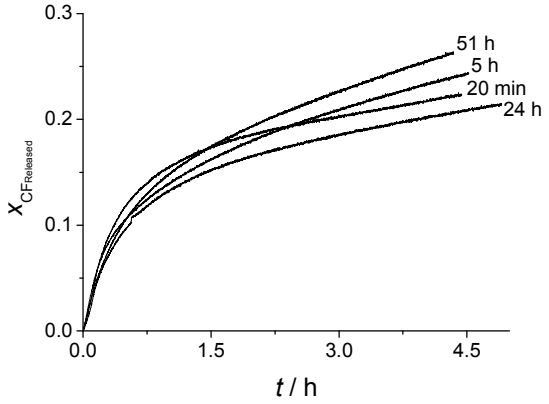


**Figure 8.** Effect of the liposome maturing time on the spontaneous leakage of CF from POPC liposomes at 25 ºC.

**Table 4.** Fitting parameters for the experimental curves displayed in Figure 8 showing the effect of the maturing time on the spontaneous leakage behaviour. Error values are the standard errors determined from the fitting procedure.

| Maturing time | $C_1'$ | $C_2'$ | $\tau_1'$ / s | $\tau_2'$ / s |
|---|---|---|---|---|
| 30 min | $-0.3458 \pm 7.55 \times 10^{-4}$ | $-0.6542 \pm 1.05 \times 10^{-4}$ | $1433.5 \pm 4$ | $1.79 \times 10^5 \pm 462$ |
| 5 h | $-0.3218 \pm 1.93 \times 10^{-3}$ | $-0.6782 \pm 1.69 \times 10^{-4}$ | $2195 \pm 10.5$ | $1.41 \times 10^5 \pm 72$ |
| 24 h | $-0.2800 \pm 6.93 \times 10^{-4}$ | $-0.7200 \pm 1.2 \times 10^{-4}$ | $1641 \pm 5.12$ | $1.70 \times 10^5 \pm 361$ |
| 51 h | $-0.281 \pm 6.45 \times 10^{-4}$ | $-0.7193 \pm 1.16 \times 10^{-4}$ | $3151 \pm 16.2$ | $1.35 \times 10^5 \pm 105$ |

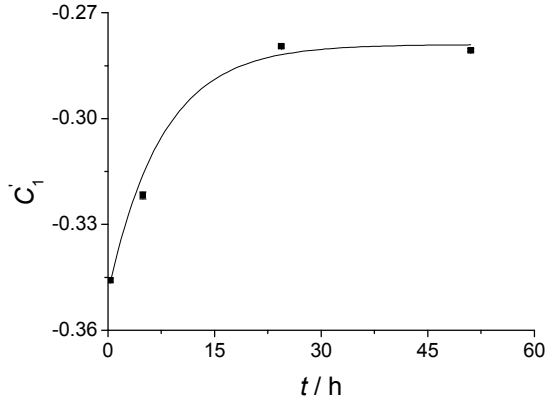


**Figure 9.** Pre-exponential factor $C_1'$ as a function of the maturing time for a POPC liposome batch kept at 25 ºC (corresponding to the same batch as Figure 8 and Table 4). The line represents the curve fitting according to equation 5 (instrumental weighting).

*3.8. Effect of the PSNPs concentration on the nucleation-inhibition kinetics*

According to equation 6, a plot of $A''$ vs. the concentration of PSNPs should result in a polynomial function of degree *n*. However, the values obtained for $A''$ present a large variation upon several repetitions at the same [PS] and the $A''$ vs. [PS] plot does not reveal any clear trend (Figure 10). The best polynomial fit without trivial parameters is obtained already for *n* = 1, i.e. a

linear fitting. However, the 95% confidence area is very broad, suggesting that the function obtained is likely to be trivial. This problem arises mainly because mechanism V assumes a single step inhibition process, when it is more likely that the formation of the inhibitor would be a sequential process, with one particle of polystyrene at a time being added to the cluster. This may account for the poor relationship between the actual and the expected trend of the $A''$ values. Modelling this process, however, results in very complex equations even if only two sequential steps are considered. The values of $k_1$ and $k_I$ are, therefore, not accesible using this approach.

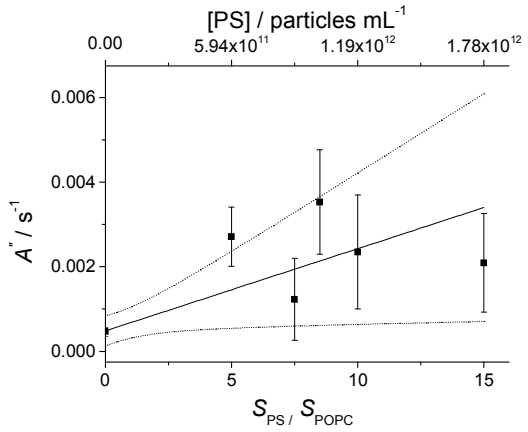


**Figure 10.** Plot of $A''$ vs. the added concentration of PSNPs ([PS]). The solid line represents the linear fit. The pointed lines delimit the 95% confidence area. Error bars are given by the standard deviation calculated from at least two repetitions of the measurements. Each point in the plot has a specific weight equal to the reciprocal of its variance (instrumental weight).

In order to be able to accept a modified version of mechanism V with a stepwise formation of the inhibitor, experimental evidence of the latter process is needed. Such evidence was obtained by determining the size distribution of the liposome-particle mixture at different times. Figure 11 shows that large clusters indeed are formed in the POPC-PSNPs mixture. These clusters become larger as the time elapses, evidencing a stepwise growth. Noteworthy, the clusters disappear upon addition of Triton X-100. This agrees with what is observed in the fluorescence measurements,

assuming that the CF release inhibitors consist of big clusters of particles encapsulating intact liposomes. The POPC lipid bilayers thus appear to act as a kind of glue, keeping the particles together. Once Triton X-100 is added, the lipid bridges interconnecting the PSNPs are destroyed; leading to a decrease in the mean cluster diameter and to the release of all the contained CF. This behavior is neither observed with pure PSNPs (Figure 11) nor with most mixtures of PSNPs with DPPC liposomes (as shown above in Figure 5). A similar tendency for cluster formation might, however, explain the large variation of the results observed upon addition of a large amount of PSNPs (15 times area excess) to DPPC liposomes (see section 3.4). The formation of clusters in POPC-PSNPs mixtures could not be readily analyzed by cryo-TEM, as the formed clusters were larger than the thickness of the vitrified sample film. Why this process is not usually observed with DPPC liposomes will be discussed in section 3.9.

| | POPC + PSNPs (1-1 area) | Pure PSNPs |
|---|---|---|
| 3 min | 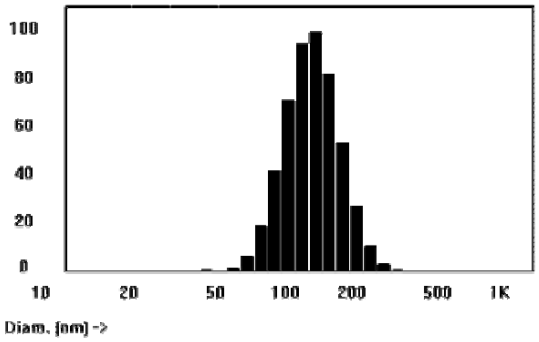 | 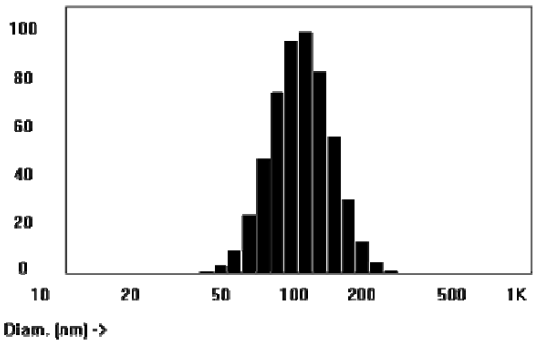 |
| 3 h | 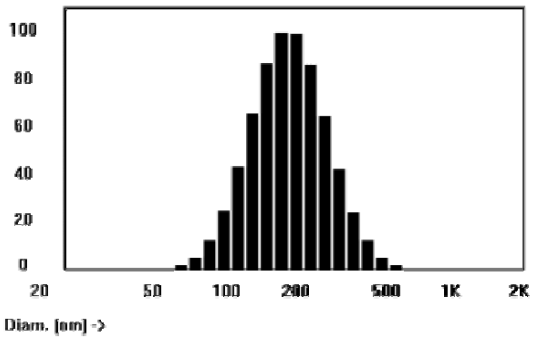 | 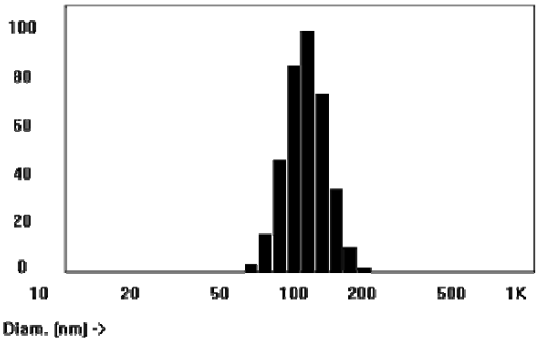 |
| 24 h | 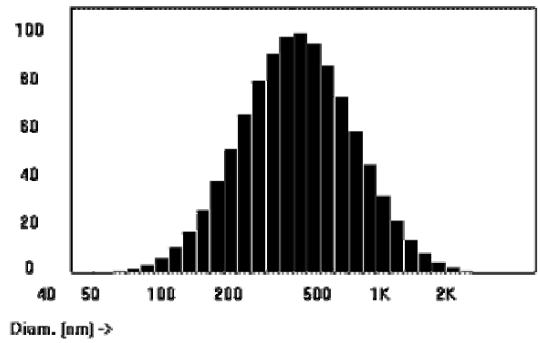 | 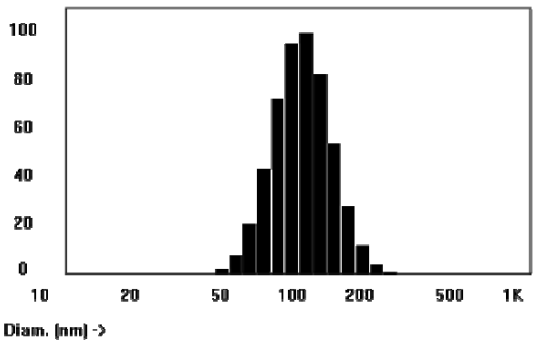 |
| 48 h | 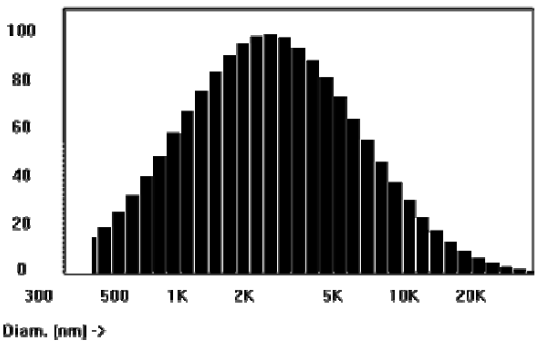 | 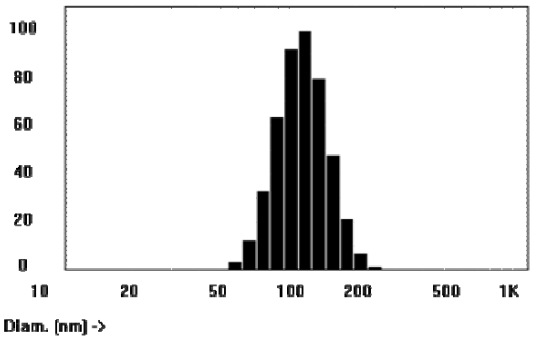 |
| After Triton X-100 | 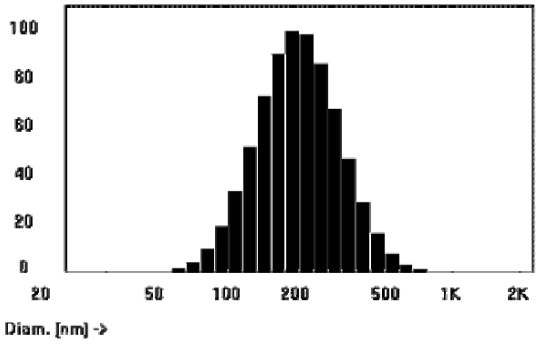 | 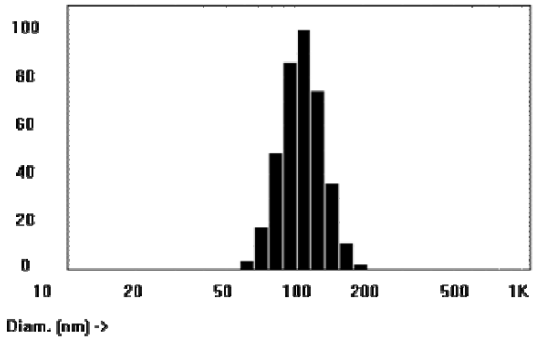 |

**Figure 11.** Size distribution as a function of time and added Triton X-100 for a 1-1 area mixture of POPC liposomes (12 μM lipid) and PSNPs and for pure PSNPs at the same concentration.

Once the existence of an activation-deactivation process in POPC liposomes is accepted, the spontaneous leakage measurements allow determining the rate constants of activation, deactivation and slow and fast spontanous leakage. The needed values are given by the relaxation constant, the limiting value $Z$ and the $A' = 4.65\times10^{-4} \pm 3.26\times10^{-5}\ s^{-1}$ and $\lambda' = 4.51\times10^{-4} \pm 3.30\times10^{-5}\ s^{-1}$ values for POPC estimated from 10 repetitions. From the fluorescence measurements for the adhesion-spreading on PSNPs, the value of $k_2'$ and rough approximations to $k_1$ and $k_I$ can be estimated. The relationships given by equation 6 provide with enough parameters to determine these values. Table 5 shows the calculated rate constants, considering $k_1$ and $k_I$ as second order rate constants. It must be recalled, however, that the actual order of these latter parameters is not known.

**Table 5.** Rate constants describing the activation-deactivation, CF spontaneous leakage and adhesion-spreading of POPC liposomes on PSNPs at 25 ºC according to the nucleation and inhibition model.

| $k_a/10^{-5}\ s^{-1}$ | $k_b/10^{-5}\ s^{-1}$ | $k_{L1}/10^{-5}\ s^{-1}$ | $k_{L2}/10^{-5}\ s^{-1}$ | $k_1$ [a]$/10^{-15}$* $[PS]^{-1}s^{-1}$ | $k_I$ [a]$/10^{-15}$* $[PS]^{-1}s^{-1}$ | $k_2'/10^{-5}s^{-1}$ | $K$ | $x_{L_i}^{eq}$ |
|---|---|---|---|---|---|---|---|---|
| 1.06 ± .387 | 2.35± .378 | 0 ± 2.34 | 43.4 ± 2.44 | 0.947 ± .206 | 1.329 ± .226 | 16 ± 3.59 | 0.451 | 0.69 |

[a][PS] given in particles*$mL^{-1}$

*3.9. Mechanism behind the formation of the CF release inhibitor*

As shown above, moderate amounts of PSNPs added to a POPC liposome suspension inhibit the release of the entrapped CF. This is not observed when employing DPPC liposome suspensions. According to the proposed nucleation-inhibition model (mechanism V) and the

discussion above, the leakage inhibitor is formed by at least one intact liposome encapsulated in a PSNPs cluster. An explanation for why such cluster formation is commonly observed with POPC liposomes while it occurs much more rarely with DPPC liposomes can be found if we examine the determined values of $x_{L}^{eq}$ and $k_{a}$ for both kinds of liposomes. Even though mechanisms II and V assume that liposomes are either active or inactive, this can be understood as just a formality employed for a more simple treatment of the kinetic equations. Actually, active liposomes may present several "degrees" of activity, i.e., different discrete amounts of active sites. In other words, a single liposome may have more than one active site. In order to comply with mechanisms II and V, the overall rate of leakage from two liposomes with one active site each should be equivalent to the total rate of leakage from one liposome with two active sites and one without. This is in fact the case as long as the CF concentration at a certain instant is the same inside all the active liposomes. As the determined values of $k_{L1}$ are very close to zero and the active sites appear and disappear on all liposomes, these assumptions can be considered to be true at any instant during the experiment. In this case, the determined value of $x_{L_a}^{eq} = 1 - x_{L_i}^{eq}$ (i.e., the fraction of active liposomes) can be interpreted as the average number of active sites expected on a liposome. The potential flaw of this interpretation of mechanisms II and V is that it makes no sense if the actual average number of active sites per liposome is close, equal or superior to 1. However, for the examples described in this report, the analyses in previous sections provide no indication that this could be the case.

To a first approximation, the distribution of active sites in the liposome population should follow the Poisson distribution, as expected for independent points distributed over equivalent portions of a surface. Using the values given in Tables 3 and 5, it is expected that in a DPPC suspension at equilibrium there will be, at any instant, approximately 0.1 % of liposomes with

two or more active sites. The corresponding value is 4% in the case of POPC liposomes. These liposomes are able to form an inhibitor instantly after addition of PSNPs, as they can immediately bind to more than one nanoparticle (single-step inhibition). The chance that an inhibitor will be instantly formed is then 40 times larger for POPC than for DPPC liposomes. Furthermore, POPC nuclei (one liposome – one particle clusters) would form new active sites faster than DPPC nuclei, as deduced from the respective $k_a$ values. This will increase their chances of recruiting new particles before rupture and spreading takes place, forming then the inhibitor cluster (stepwise inhibition).

## 4. Conclusions

The discussion above shows that liposome suspensions, both in the gel and the liquid crystalline phase state, present a dynamic exchange between fast leaking (active) and slow leaking (inactive) liposome populations that cannot be diferentiated from one another by usual means. These two populations behave differently when a hydrophobic surface is present: while the fast leaking liposomes display affinity for the surface, the slow leaking liposomes do not. The reported fact (both in this and in previous publications[44,48]) that eventually all liposomes close to the surface will adhere to it, is explained by means of the dynamic activation-deactivation described here. It is proposed that the difference between active and inactive liposomes is the presence or absence, respectively, of a critical amount of hydrophobic defects in the lipid bilayer membrane. Further research is required to assess the exact nature of these defects.

The dynamic exchange between active and inactive liposomes eventually leads to an equilibrium composition of the suspension. However, it is expected that most fresh liposome preparations will contain a higher than equilibrium proportion of active liposomes. This translates into a risk for inaccuracies and irreproducibility in experiments based on the measurement of

liposome spontaneous leakage or involving the interaction of liposomes with surfaces or solutes. Different groups have, for example, reported dissimilar CF leakage rates from liposomes of the same composition (pure DPPC among them) and under the same conditions[49-51]. To our knowledge, the model proposed here is the first one to address these discrepancies beyond pure speculation. The current report shows the importance of considering the liposome age and acquiring knowledge concerning the activation-deactivation conditions, in order to assure that a certain liposome suspension is found in equilibrium and therefore can produce reproducible results. Data presented here show that up to 12 hours are needed in order for the DPPC suspension to reach a proportion of inactive liposomes equal to 95% of the amount found under equilibrium conditions (or 20 hours for 99%). For the case of POPC, the time increases to 25 hours (39 hours for 99%). Further research is being carried out in order to determine if the same phenomenom is observed for liposomes containing, among others, charged lipids, polyethylene glycol (PEG) headgroups and/or cholesterol.

Another important implication of the results presented here is that, if the activation-deactivation process is understood, it can potentially be controlled to produce a suspension with a large majority of the desired liposomes (active or inactive).

The fact that two populations of liposomes with different affinity for surfaces and solutes are present in potentially all liposome suspensions must also be considered when analyzing experimental data. Even if the equilibrium condition has been reached, the different behaviors of active and inactive liposomes, as well as the dynamic exchange between them must be taken into account. This need is illustrated, for example, by a report by Johnson et al.[52], who observed than in a supposedly homogeneous liposome suspension some liposomes adhered and spread immediately on a quartz surface while others did it stepwise. More recently, Woodward et al.[48] found that the number of liposomes that adhere and spread on a hydrophobic alkanethiol self-

assembled monolayer is significantly lower than the number of liposomes reaching the surface. This observation contradicts the available evidence stating that all liposomes reaching the substrate are present near the surface and eventually adhere and spread[31]. The authors interpreted this discrepancy as a lag between the time at which the liposome associates with the surface and when it organizes to form a spread lipid monolayer. Also, Agmo Hernández et al.[44] showed that a reversible reaction should precede the adhesion and spreading of liposomes on mercury. Although punctual explanations for these specific observations have been proposed, they all can be more generally understood if considered in the framework of the activation-deactivation equilibrium proposed in this report.

In short, it is necessary to be aware of the activation-deactivation dynamic exchange occurring in liposome suspensions in order to a) obtain reliable and reproducible experimental data and b) get a better understanding of processes involving the lipid membrane.

**Acknowledgements**

Financial support from the Swedish Research Council and the Swedish Cancer Society is gratefully acknowledged.

**References**

(1) Boija, E.; Lundquist, A.; Edwards, K.; Johansson, G. *Anal. Biochem.* **2007**, *364*, 145-152.

(2) Johansson, E.; Engvall, C.; Arfvidsson, M.; Lundahl, P.; Edwards, K. *Biophys. Chem.* **2005**, *113*, 183-192.

(3) Ng, C. C.; Cheng, Y. L.; Pennefather, P. S. *Biophys. J.* **2004**, *87*, 323-331.

(4) Li, S.; Palmer, A. F. *Langmuir* **2004**, *20*, 4629-4639.

(5) Fielding, R. M.; Lasic, D. D. *Expert Opin. Ther. Pat.* **1999**, *9*, 1679-1688.

(6) Lasic, D. D.; Papahadjopoulos, D. *Current Opin. Solid St. M.* **1996**, *1*, 392-400.

(7) Lasic, D. D.; Templeton, N. S. *Adv. Drug Deliver. Rev.* **1996**, *20*, 221-266.

(8) Lasic, D. D. *Trends Biotechnol.* **1998**, *16*, 307-321.

(9) Templeton, N. S.; Lasic, D. D. *Mol. Biotechnol.* **1999**, *11*, 175-180.

(10) Brian, A. A.; McConnell, H. M. *P. Natl. Acad. Sci.-Biol.* **1984**, *81*, 6159-6163.

(11) Sackmann, E. *Science* **1996**, *271*, 43-48.

(12) Stauffer, V.; Stoodley, R.; Agak, J. O.; Bizzotto, D. *J. Electroanal. Chem.* **2001**, *516*, 73-82.

(13) Richter, R. P.; Bérat, R.; Brisson, A. R. *Langmuir* **2006**, *22*, 3497-3505.

(14) Keller, C. A.; Kasemo, B. *Biophys. J.* **1998**, *75*, 1397-1402.

(15) Lüthgens, E.; Herrig, A.; Kastl, K.; Steinem, C.; Reiss, B.; Wegener, J.; Pignataro, B.; Janshoff, A. *Meas. Sci. Technol.* **2003**, *14*, 1865-1875.

(16) Reiss, B.; Janshoff, A.; Steinem, C.; Seebach, J.; Wegener, J. *Langmuir* **2003**, *19*, 1816-1823.

(17) Rodahl, M.; Hook, F.; Fredriksson, C.; Keller, C. A.; Krozer, A.; Brzezinski, P.; Voinova, M.; Kasemo, B. *Faraday Discuss.* **1997**, *107*, 229-246.

(18) Keller, C. A.; Glasmastar, K.; Zhdanov, V. P.; Kasemo, B. *Phys. Rev. Lett.* **2000**, *84*, 5443-5446.

(19) Jass, J.; Tjärnhage, T.; Puu, G. *Biophys. J.* **2000**, *79*, 3153-3163.

(20) Jenkins, A. T. A.; Bushby, R. J.; Evans, S. D.; Knoll, W.; Offenhäusser, A.; Ogier, S. O. *Langmuir* **2002**, *18*, 3176-3180.

(21) Liang, X. M.; Mao, G. Z.; Ng, K. Y. S. *J. Colloid. Interf. Sci.* **2004**, *278*, 53-62.

(22) Liang, X. M.; Mao, G. Z.; Ng, K. Y. S. *Colloid. .Surface. B* **2004**, *34*, 41-51.

(23) Tero, R.; Watanabe, H.; Urisu, T. *Phys. Chem. Chem. Phys.* **2006**, *8*, 3885-3894.

(24) Teschke, O.; de Souza, E. F. *Langmuir* **2002**, *18*, 6513-6520.

(25) Winger, T. M.; Chaikof, E. L. *Langmuir* **1998**, *14*, 4148-4155.

(26) Kunneke, S.; Kruger, D.; Janshoff, A. *Biophys. J.* **2004**, *86*, 1545-1553.

(27) Wong, J. Y.; Park, C. K.; Seitz, M.; Israelachvili, J. *Biophys. J.* **1999**, *77*, 1458-1468.

(28) Nissen, J.; Gritsch, S.; Wiegand, G.; Radler, J. O. *Eur. Phys. J. B* **1999**, *10*, 335-344.

(29) Yuan, J.; Parker, E. R.; Hirst, L. S. *Langmuir* **2007**, *23*, 7462-7465.

(30) Liu, K. W.; Biswal, S. L. *Anal. Chem.* **2010**, *82*, 7527-7532.

(31) Hubbard, J. B.; Silin, V.; Plant, A. L. *Biophys. Chem.* **1998**, *75*, 163-176.

(32) Silin, V. I.; Wieder, H.; Woodward, J. T.; Valincius, G.; Offenhausser, A.; Plant, A. L. *J. Am. Chem. Soc.* **2002**, *124*, 14676-14683.

(33) Tawa, K.; Morigaki, K. *Biophys. J.* **2005**, *89*, 2750-2758.

(34) Hernandez, V. A.; Scholz, F. *Israel J. Chem.* **2008**, *48*, 169-184.

(35) Radler, J.; Strey, H.; Sackmann, E. *Langmuir* **1995**, *11*, 4539-4548.

(36) Williams, L. M.; Evans, S. D.; Flynn, T. M.; Marsh, A.; Knowles, P. F.; Bushby, R. J.; Boden, N. *Langmuir* **1997**, *13*, 751-757.

(37) Sek, S.; Xu, S.; Chen, M.; Szymanski, G.; Lipkowski, J. *J. Am. Chem. Soc.* **2008**, *130*, 5736-5743.

(38) Li, M.; Chen, M.; Sheepwash, E.; Brosseau, C. L.; Li, H.; Pettinger, B.; Gruller, H.; Lipkowski, J. *Langmuir* **2008**, *24*, 10313-10323.

(39) Lipkowski, J. *Phys. Chem. Chem. Phys.* **2010**, *12*, 13874-13887.

(40) Hellberg, D.; Scholz, F.; Schubert, F.; Lovric, M.; Omanovic, D.; Hernandez, V. A.; Thede, R. *J. Phys. Chem. B* **2005**, *109*, 14715-14726.

(41) Hernandez, V. A.; Scholz, F. *Langmuir* **2006**, *22*, 10723-10731.

(42) Hernandez, V. A.; Scholz, F. *Bioelectrochemistry* **2008**, *74*, 149-156.

(43) Hernandez, V. A.; Milchev, A.; Scholz, F. *J. Solid State Electr.* **2009**, *13*, 1111-1114.

(44) Hernandez, V. A.; Hermes, M.; Milchev, A.; Scholz, F. *J. Solid State Electr.* **2009**, *13*, 639-649.

(45) Milchev, A. *Russ. J. Electrochem.* **2008**, *44*, 619-645.

(46) DeNardis, N. I.; Zutic, V.; Svetlicic, V.; Frkanec, R.; Tomasic, J. *Electroanal.* **2007**, *19*, 2444-2450.

(47) Almgren, M.; Edwards, K.; Karlsson, G. *Colloid. Surface. A* **2000**, *174*, 3-21.

(48) Woodward, J. T.; Meuse, C. W. *J. Colloid. Interf. Sci.* **2009**, *334*, 139-145.

(49) Barbet, J.; Machy, P.; Truneh, A.; Leserman, L. D. *Biochim. Biophys. Acta* **1984**, *772*, 347-356.

(50) Straubinger, R. M.; Hong, K.; Friend, D. S.; Papahadjopoulos, D. *Cell* **1983**, *32*, 1069-1079.

(51) Szoka, F. C.; Jacobson, K.; Papahadjopoulos, D. *Biochim. Biophys. Acta* **1979**, *551*, 295-303.

(52) Johnson, J. M.; Ha, T.; Chu, S.; Boxer, S. G. *Biophys. J.* **2002**, *83*, 3371-3379.

**For TOC only**